Title

Local field potentials identify features of cortico-hippocampal communication impacted by stroke and environmental enrichment therapy.

Journal

Journal of Neural Engineering, 18(4)

ISSN

1741-2560

Authors

Ip, Zachary
Rabiller, Gratianne
He, Ji-Wei
et al.

Publication Date

2021-08-01

DOI

10.1088/1741-2552/ac0a54

Peer reviewed

HHS Public Access

Author manuscript

J Neural Eng. Author manuscript; available in PMC 2022 January 06.

Published in final edited form as:

J Neural Eng. ; 18(4): . doi:10.1088/1741-2552/ac0a54.

Local Field Potentials identify features of cortico-hippocampal communication impacted by stroke and environmental enrichment therapy

Zachary Ip, B.S.[1], **Gratianne Rabiller, PhD.**[2,3], **Ji-Wei He, PhD.**[2,3], **Shivalika Chavan, High School Diploma**[1], **Yasuo Nishijima, M.D.,PhD.**[2,3,4], **Yosuke Akamatsu, M.D.,PhD.**[2,3,5], **Jialing Liu, PhD.**[2,3], **Azadeh Yazdan-Shahmorad, PhD.**[1,6]

[1.]Department of Bioengineering, University of Washington, Seattle, WA, USA

[2.]Department of Neurosurgery, University of California San Francisco, San Francisco, CA 94158, USA

[3.]San Francisco VA medical center, San Francisco, CA 94121, USA

[4.]Department of Neurosurgery, Tohoku University Graduate School of Medicine[3], 1-1 Seiryo-machi, Aoba-ku, Sendai 980-8574, Japan

[5.]Department of Neurosurgery, Iwate Medical University, 1-1-1 Idaidori, Yahaba, Iwate, 028-3694, Japan

[6.]Department of Electrical and Computer Engineering, University of Washington, Seattle, WA, USA

Abstract

Objective—Cognitive and memory impairments are common sequelae after stroke, yet how middle cerebral artery (MCA) stroke chronically affects the neural activity of the hippocampus, a brain region critical for memory but remote from the stroke epicenter, is poorly understood. Environmental enrichment (EE) improves cognition following stroke; however, the electrophysiology that underlies this behavioral intervention is still elusive.

Approach: We recorded extracellular local field potentials simultaneously from sensorimotor cortex and hippocampus in rats during urethane anesthesia following MCA occlusion and subsequent EE treatment.

Main results: We found that MCA stroke significantly impacted the electrophysiology in the hippocampus, in particular it disrupted characteristics of sharp-wave associated ripples (SPW-Rs) altered brain state, and disrupted phase amplitude coupling (PAC) within the hippocampus and between the cortex and hippocampus. Importantly, we show that EE mitigates stroke-induced changes to SPW-R characteristics but does not restore hippocampal brain state or PAC.

Corresponding Author: Azadeh Yazdan-Shahmorad, UW Bioengineering, UW Mailbox 355061, Seattle WA 98195, azadehy@uw.edu, +1 (415) 351-9744.

Conflict of interest statement: The authors declare no competing financial interests.

Significance: These results begin to uncover the complex interaction between cognitive deficit following stroke and EE treatment, providing a testbed to assess different strategies for therapeutics following stroke.

Introduction:

Stroke is a leading cause of adult disability, with the most common occurrence in the middle cerebral artery (MCA) region in humans. Unfortunately, there are few effective treatment options for disability following stroke. In addition to the impairment of high-level sensorimotor functions, a common outcome of stroke is cognitive and memory deficit[1]. The hippocampus is highly involved in the encoding and retrieval of memories, but hippocampal and parahippocampal areas are rarely directly affected by MCA stroke because hippocampal blood flow is supplied by the posterior circulation[2]. Animal models represent this phenomenon, displaying cognitive impairment following stroke in the absence of hippocampal injury[3,4]. However, a thorough understanding of the mechanisms underlying cognitive and memory impairment caused by MCA stroke remains poorly understood.

Cortical dysfunction following MCA stroke is well described by histological and electrophysiological methods[5,6]. Hippocampal functional impairment following MCA stroke has been demonstrated using behavioral assessment[3], however how hippocampal electrophysiology changes following stroke is largely unknown. There are many hippocampal electrophysiological features correlated with memory such as the ratio of theta to delta (TD) band signal power of the CA1 pyramidal layer within the hippocampus which defines brain states relevant to memory function[7]. High theta/delta ratio (HTD) during sleep, also known as rapid eye movement sleep, is correlated with memory performance [8]. Manipulation of hippocampal HTD alters cognition, further supporting HTD's role in cognition[7,9]. Meanwhile, low theta/delta ratio (LTD), also known as slow wave state, is associated with immobility and memory consolidation. SPW-Rs are short, high frequency oscillations that represent memory recall and encoding[10], which occur during LTD and in the awake state during consummation and immobility[11].

Theta oscillations in the hippocampus provide a temporal reference for gamma oscillations through theta-gamma coupling[12] which can be measured using phase amplitude coupling (PAC)[13]. Theta-gamma coupling within the hippocampus supports memory processes during HTD[12,14]. PAC has been observed between brain regions such as the prefrontal and entorhinal cortex[15,16]. Manipulating theta has been shown to alter cognition[17], further supporting theta oscillation's causative role in cognition.

Chronic stroke leads to a complex cascade of effects within the brain such as the loss of functional connectivity[18] and changes in local oscillations[19,20], which can affect remote brain areas such as the hippocampus. EE is an effective non-invasive therapy that has long been studied as a potential treatment for improving cognition[21] by increasing exposure to novelty, social contact, and physical activity. Cognitive and behavioral deficit following stroke is consistently improved by environmental enrichment (EE)[3,22–24]. However, the underlying electrophysiological mechanisms are still largely unknown.

We have previously shown that an MCA occlusion acutely disrupts the electrophysiology of the hippocampus, which we observed through increases in SPW-R frequency and theta-gamma coupling between hippocampus and cortex within the first hour of ischemia[25]. Here we seek to understand the changes in hippocampal electrophysiology during chronic phase of MCA stroke to understand the underlying mechanisms of cognitive impairment following stroke and cognitive improvement following EE.

Materials & Methods:

A. Animals

We conducted all experiments in accordance with the animal care guidelines issued by the National Institutes of Health and by the San Francisco VA Medical Center Institutional Animal Care and Use Committee. We used adult male Sprague-Dawley rats approximately 2.5 months of age weighing 250g (Charles River Laboratories, Wilmington, MA) housed in institutional standard cages (2 rats per cage) on a 12-hr light/12-hr dark cycle with ad libitum access to food and water before the experimental procedures. Only male rats were used to avoid potential effect of sex hormones on stroke injury. The identity of the test subject was blinded to investigators who performed the stroke surgery and recording.

B. Experimental Stroke

Stroke was induced unilaterally in rats by the distal MCA occlusion method in combination with supplemental proximal artery occlusion of the bilateral common carotid arteries under isoflurane (1.5%)/O2(30%)/N2O(68.5%) anesthesia as described previously[25,26], producing cortical infarct restricted to the somatosensory cortex[3]. Core temperature was maintained at 37±0.5 °C with a heating blanket and rectal thermistor servo loop throughout the procedure. Mortality due to stroke was approximately 12–15%.

C. Environmental Enrichment

Immediately following MCA occlusion, we randomly assigned rats into EE or standard housing groups. One week after surgery, we transferred the EE group rats to EE cages (dimensions: 76 × 56 × 77 cm; 2-story cage equipped with a running wheel, a 3-dimensional labyrinth, bedding, a ladder, a house, chains, a hammock, wooden blocks, and nylon bones; 10 rats per cage) for 3 weeks of residence. Similarly, non-stroke control animals assigned to EE treatment were placed in EE cages for 3 weeks before recording. We changed the arrangement of movable objects once a week to maintain novelty[3,23]. Rats assigned to the standard housing groups remained in institutional standard cages.

D. Recording

We performed electrophysiological recordings using two 16-site extracellular silicon probes (NeuroNexus Technologies) under urethane anesthesia for two hours (Sigma, 15 mg/kg i.p.). Following craniotomy, 2 electrodes (A1×16–5mm-100–703) were inserted into each hemisphere after the dura mater was pierced to target the dorsal hippocampus at AP: −3.3 mm; ML: +/− 2 mm via a stereotaxic frame (David Kopf Instruments, Tujunga, CA, USA) (Figure 1). Real-time data display and an audio aid were used to facilitate the identification of proper recording location while advancing electrodes until characteristic signals from

stratum pyramidal and stratum radiatum were detected and recorded. We collected a 2-hr multi-channel recording from bilateral sensorimotor cortex and dorsal hippocampus from each rat. Data were stored at a sampling rate of 32 kHz after band-pass filtering (0.1–9 kHz) with an input range of ± 3 mV (Digital Lynx SX, Neuralynx, USA). We down sampled all recordings to 1250 Hz (Matlab, MathWorks, USA) prior to analysis. Approximately 7–10% of rats were excluded due to excessive bleeding occurred during craniotomy surgery or insertion of recording or reference electrodes.

E. Tissue preparation and infarct assessment

After recording, rats were perfused transcardially with 4% paraformaldehyde in 0.1M phosphate buffer, pH 7.4. The brains were collected, post fixed overnight in 4% PFA, and placed in 30% sucrose solution for 24 h. Brains were cut coronally in 40 m-thick sections and stored at 4°C. Serial coronal sections were stained using the hematoxylin and eosin method. Infarct volume was measured by subtracting the difference between intact tissue in the ipsilesional side from the contralesional side using Stereoinvestigator software (Microbrighfield, VA). We determined both the infarct volume and the ratio of infarct to intact tissue volume[4].

F. Data Analysis

We used local field potentials (LFP) from deep cortical layers and four layers from CA1 field hippocampus (stratum oriens, pyramidal, radiatum and lacunosum-moleculare) in our analysis. We isolated brain waves from the LFPs by band-pass filtering the following frequency ranges: delta (0.1–3 Hz), theta (4–7 Hz), alpha (7–13 Hz), beta (13–30 Hz), gamma (30–58 Hz), and high-gamma (62–200 Hz). A total of 52 rats were successfully recorded and subjected to data processing. We further excluded the data from 10 rats after screening for bad channels and recordings where individual layers could not be discerned. The groups had the following counts: control (n=8), enriched control (EEC) (n=10), two-week stroke (2WS) (n=6), one-month stroke (1MS) (n=9) and enriched one-month stroke (EES) (n=9). To analyze changes to signal power we normalized data by subtracting the mean and dividing by the standard deviation to account for impedance differences between individual electrodes.

To estimate LTD and HTD brain states we calculated the ratio of spontaneous signal power between theta band and delta band from the pyramidal layer. The threshold defining LTD and HTD states was defined manually for each animal by visual assessment[27,28]. The ratio of HTD/LTD was calculated by dividing the total time spent in each state for each recording.

SPW-Rs were identified when a pyramidal ripple and radiatum sharp wave co-occurred as described previously[11,28]. To detect pyramidal ripples, the LFP of the pyramidal layer was bandpass filtered (150–250 Hz), then squared and Z-scored. When the signal exceeded 6 standard deviations for a period longer than 20 ms, an event was registered. When the signal subsequently dropped below 1 SD, the event was considered ended. To identify radiatum sharp waves, a similar process was used, however the bandpass filter was from 8 to 40 Hz, and the standard deviation threshold was 3.

We performed laminar current-source density (CSD) analysis[29] along each electrode, temporally aligning the LFP to the onset of a SPW-R, and spatially centering each recording on the pyramidal layer. We used windows of time before during and after ripple to examine local current flow in relation to the timing of ripple firing. Dipole amplitude was calculated by finding the maximum and minimum current along the probe from the specified time window and taking the difference. We analyzed PAC within the hippocampus and between the layers of the hippocampus and the cortex as a metric of functional connectivity and communication. PAC was calculated as described in[13]. Briefly, we bandpass filtered the LFP between (0.1–200 Hz), extracted and the instantaneous phase and amplitude using the Hilbert transform. A composite phase-amplitude time series then determined the amplitude distribution across phase. The modulation index (MI) is then calculated from the divergence of the amplitude distribution from a uniform distribution[13]. MI was compared between groups by averaging the MI across a window of frequencies pertaining to canonical frequency bands. A data driven threshold was found using Otsu's method[30] to determine the window of significant coupling.

G. Statistical analysis

We expressed data as mean ±standard error. We performed one-way ANOVA to assess changes in stroke progression, and two-way ANOVA to assess changes between the effect of stroke and the effect of EE. We used post-hoc Bonferroni's to control for multiple comparisons between treatment groups. We performed between-group comparisons for each neural feature independently. We performed paired t-tests to assess changes between hemispheres. For non-normal distributions, we performed Kruskal-Wallis with post-hoc Bonferroni's to control for multiple comparisons. We considered p values less than 0.05 as significant.

Results:

We analyzed the absolute infarcted volume and the ratio of infarcted volume to intact tissue volume, confirming there was no hippocampal lesion and determining whether lesion size was affected by the chronicity of stroke or by exposure to enrichment. There was no apparent morphological difference in the hippocampus as revealed by hematoxylin and eosin staining between the stroke and non-stroke groups, suggesting that experimental MCA did not compromise hippocampal structural integrity. Both analyses revealed that lesion size did not significantly differ between groups (ANOVA; $p<0.460$) (Supplemental Figure 1). We verified probe location through histology, spanning from −3mm to −3.72mm AP and 2.5mm to 3mm laterally (Figure 1).

We analyzed normalized signal power within the cortex and hippocampus as a simple metric of activity levels within the tissue. Surprisingly, there were sparse significant differences between groups. Delta power in 2WS and 1MS tended to be lower than control in both cortex and hippocampus, though interestingly, theta, gamma and high gamma signal power tended to be higher in both 2WS and 1MS compared to control (Figure S2).

Brain state stability is disrupted following stroke

We analyzed the stability of TD states under anesthesia by analyzing the duration of HTD state (Figure 2A). Surprisingly, we found that TD state stability is disrupted following stroke despite no direct lesion to the hippocampus, with a significant decrease in the duration of HTD brain state bilaterally for both stroke groups compared to control (ANOVA; $p<3.33e-4$) (Figure 2B, Figure S3A). However, the disruption of state stability does not alter the overall proportion of HTD to LTD as evidenced by the HTD/LTD ratio (Figure 2C, Figure S3B) (ANOVA; $p>0.21$). This shows that stroke chronically disrupts the stability of brain states defined within the hippocampus, but does not disrupt the proportion of HTD to LTD.

SPW-R characteristics change following stroke

SPW-Rs occur within the CA1 pyramidal layer of the hippocampus during LTD and represent memory encoding. We quantified characteristics of SPW-Rs following stroke. There was an increase in SPW-R signal power of both ipsilesional and contralesional hemispheres in 2WS and 1MS compared to control (Kruskal Wallis; $p<9.97e-4$) (Figure 3A, Figure S4A). The duration of SPW-Rs was also significantly different; SPW-Rs at 2WS were significantly longer than control (ANOVA; $p=5.41e-5$), while SPW-Rs at 1MS were significantly shorter (ANOVA; $p=5.41e-5$) (Figure 3B). These results indicate that stroke significantly affects both power and duration of SPW-Rs. Both the signal power and duration of SPW-Rs at 2WS significantly increased compared to 1MS in both hemispheres (Kruskal Wallis; $p<4.03e-9$,). These results indicate that there is some compensatory mechanism occurring at 2WS.

Current flow surrounding SPW-Rs is disrupted following stroke

We performed laminar CSD aligned to the onset of SPW-R to evaluate current flow through the hippocampus during SPW-Rs. The control group revealed pairs of dipoles with the apparent source centered in the pyramidal layer with the sink centered in the radiatum as expected. After SPW-R, the dipole reverses at a lower amplitude, with the sink in pyramidal and the source in the radiatum (Figure 4A). This post-SPW-R phase lasts approximately 0.6 seconds before dissipating. To analyze these changes to this current flow, we calculated the amplitude of current within windows of interest before, during, and after SPW-R.

In both hemispheres, the dipole amplitude before, during, and after SPW-R was significantly higher at 2WS compared to control (ANOVA; $p<0.0077$) (Figure 4B, Figure S5) while the amplitude of 1MS is significantly lower compared to control (ANOVA; $p<6.78e-4$,) (Figure 4B). Like SPW-R power and duration, the dipole amplitude at 1MS is significantly lower than 2WS before, during and after SPW-R (ANOVA; $p<4.72e-5$). These results show that stroke causes significant change in current flow, while the decrease of dipole amplitude from 2WS to 1MS support our SPW-R previous observations that there is some compensatory activity at 2WS.

Theta-gamma coupling between hippocampus and cortex is reduced following stroke

Theta rhythms coordinate high frequency gamma activity within the hippocampus during HTD and supports memory processes. We used PAC to detect theta-gamma coupling within the hippocampus, and to determine whether coupling existed between cortex and

hippocampus. During HTD, theta-gamma coupling, and delta-high gamma coupling was present bi-directionally within the hippocampus as expected, however we also detected coupling between cortex and hippocampus in the control group. Coupling within the pyramidal layer and between pyramidal theta and cortical gamma are shown as examples (Figure 5A). Although the majority of coupling is captured by the theta frequency band, some coupling extends to the border between theta and delta (Figure S6), however for the rest of the analysis we are focusing on theta-gamma coupling. Ipsilesional coupling within the pyramidal layer was significantly lower at 1MS compared to control. Interestingly, ipsilesional coupling between hippocampus and cortex at 1MS was also significantly lower than control for all hippocampal layers in compared to control (Figure 5B) (ANOVA; $p<0.0356$). Coupling within the hippocampus and between cortex and hippocampus is lower than control at 2WS, though not significantly. This could be due in part to the compensatory mechanisms observed in SPW-Rs. During LTD, theta-gamma coupling was not present within the cortex or between cortex and hippocampus as expected. Instead, only delta-high gamma coupling was present during LTD, which did not change following stroke. The breakdown in PAC between hippocampal theta and cortical gamma implies that MCA stroke, which does not cause infarct to the hippocampus, breaks down coordination of oscillations between theta and gamma within the hippocampus, and the coordination of cortical gamma by hippocampal theta.

The effect of Environmental Enrichment on stroke

Following our analysis of stroke progression, we investigated the effect of EE on the hippocampal electrophysiological features involved in memory using a two-way ANOVA. EE had two main interactions with these features affected by stroke. Characteristics of SPW-Rs, which were increased by stroke, were mitigated by EE. Interestingly, features that were disrupted by stroke, such as TD state and PAC, were further disrupted by EE.

To analyze the effect of EE on hippocampal features of memory, we first looked at characteristics of SPW-Rs. We started with SPW-R power. At 1MS SPW-R power is significantly higher than control in both hemispheres, (Figure 6A) (ANOVA; $p<2.16e-4$), while there is no significant difference between control, EES, and EEC (ANOVA; $p>0.058$). SPW-R power show that EE mitigates the effects following stroke.

We then analyzed the duration of SPW-Rs. At 1MS the duration of SPW-Rs is significantly shorter than control ipsilesionally (ANOVA; $p=5.65e-5$), while control, EES, and EEC are not significantly different (ANOVA; $p=1$) (Figure 6B). Contralesionally, the duration of 1MS, EEC, and EES are all significantly shorter than control (Figure S8B) (ANOVA; $p<2.61e-10$), though 1MS is also significantly shorter than EES. Like SPW-R power, SPW-R duration results show that EE mitigates the decrease in duration following stroke. These results support our findings in SPW-R power that EE tends to reduce the severity of the effects of stroke.

As for the effects on the CSD surrounding SPW-Rs, we see that stroke generally causes an increase in dipole amplitude, while EE generally causes a decrease in dipole amplitude. Leading up to SPW-R, there is a between-subjects effect in both the ipsilesional and contralesional hemisphere for stroke (ANOVA; $p<2.09e-6$) (Table S1). The dipole amplitude

ipsilesionally at 1MS is significantly higher than EEC and EES before, during, and after SPW-R (ANOVA; $p<1.77e-5$), while there is no significant difference between control, EEC, and EES (ANOVA, $p>0.15$) (Figure 6C). These changes support our findings that EE mitigates the effects of stroke.

Investigating the effect of EE on TD states revealed a between-subjects effect that both stroke and EE significantly decrease the length of ipsilesional HTD state (ANOVA; $p<0.0041$), though contralesionally, only stroke significantly changed HTD state (ANOVA; $p=3.01e-6$) (Table S1). This was shown in our post-hoc analysis as well, where the length of ipsilesional HTD in 1MS, EEC, and EES were all significantly lower than control (ANOVA; $p<0.021$) (Figure 6D). Neither stroke nor EE had any significant effect on the ratio of HTD/LTD (Figure 6E, Table S1). These results show that both EE and stroke can disrupt the stability of TD states, while leaving the ratio of HTD/LTD intact.

Contrary to its known benefit on synaptic plasticity and cognition, EE unexpectedly lowered the levels of theta-gamma coupling during HTD. The between-subjects effects show both stroke and EE significantly lower ipsilesional and contralesional theta-gamma coupling. Additionally, stroke and EE showed significant interaction ipsilesionally, meaning that the change in PAC seen in EES compared to control was significantly different than could be expected from the additive effects of stroke and EE combined (ANOVA; $p<0.017$) (Figure 6F, Table S1). Our post-hoc analysis revealed that coupling in 1MS, EEC, and EES are all significantly lower than control ipsilesionally (ANOVA; $p<2.10e-4$), while contralesionally coupling in 1MS and EES are significantly lower than control (ANOVA; $p<0.0022$) (Figure S8F). These results additionally show a reduction of information flow between cortico-hippocampal networks for both stroke and EE groups.

Discussion:

While impairment of memory after dMCAO is well reported, (e.g. poor performance in the Barnes Maze test and hippocampal hypoactivation following spatial exploration[3)], the electrophysiological substrates of cognitive deficit in the hippocampus have not been established. There are no direct projections between the sensorimotor cortex and hippocampus. However, we recently showed that cortical lesion following dMCAO stroke acutely affects the electrophysiology of the hippocampus. We saw counterintuitive effects, such as an increase in SPW-Rs, an increase in theta-gamma coupling, and a persistent increase in LTD state[25]. These results showed that MCA stroke strongly affects remote regions like the hippocampus. With these neural features, we sought to understand the underlying changes to hippocampal electrophysiology that drive the cognitive deficit observed during chronic phase of stroke, and how EE interacts with these effects.

We found that EE mitigates the stroke induced changes to SPW-R characteristics, like SPW-R power, duration, and CSD. This shows that although the anatomy of the hippocampus is not compromised, SPW-Rs, which are well known and thoroughly studied for their role in memory and cognition, are disrupted throughout stroke progression. Crucially, we show that EE stabilizes the characteristics of SPW-Rs throughout stroke progression, revealing that EE impacts features related to cognition. These results begin to uncover the complex interaction

between stroke and EE, providing a testbed to assess different strategies for therapeutics following stroke. Our recordings allowed analysis of other features as well. For features such as TD brain state and PAC, EE compounded the disruptions caused by stroke. These neural features may be areas of interest to further understand the network imbalances caused by stroke and to investigate future therapeutic interventions.

PAC has been characterized within the hippocampus in previous work[14–16]. Interestingly, the frequency range defining theta in these studies has been inconsistent (e.g. 7–12 Hz[14], 4–12 Hz[15], and 6–10 Hz[16]). Crucially, the coupling that we are seeing in our results here is the lower than these frequencies (3–5 Hz) (Figure S6). The neural activity from previous studies were recorded during awake behaving sessions; therefore, the coupling at lower frequencies that we observe here maybe due to urethane anesthesia. To our knowledge this is the first time PAC is being reported between cortex and hippocampus where we also see coupling of gamma to lower frequencies (3–5 Hz) consistent with the range we see within hippocampus.

Current literature describes stroke progression as two opposing phases. The first phase lasts approximately three days after onset, characterized by increased activity and plasticity, and excitotoxic cell death. Following this, neuronal activity is chronically suppressed[31]. Our results show that SPW-Rs, which encode memories within the hippocampus, remain upregulated up to two weeks before partially retuning to baseline levels, while TD state and PAC are chronically disrupted.

The chronic changes to hippocampal electrophysiology differ drastically from the acute effects occurring in the hour after infarct, detailed in[25]. The frequency of SPW-Rs increases in the acute setting, while in the chronic setting SPW-R power increases at 2WS. PAC also differs between acute and chronic settings, where theta gamma coupling is increased in the acute setting and disrupted in the chronic setting.

SPW-Rs are well-known for their causative role in memory performance: disruption on SPW-Rs interferes with memory formation[11]. The marked increase in SPW-R power, duration, and current flow at 2WS may be correlated with the increased cortical plasticity or disinhibition during stroke progression. This suggests some compensatory activity at 2WS. The decrease in SPW-R power, duration, and current flow at 1MS could represent stabilization of the network. Long-duration SPW-Rs are correlated with increased memory function[32], which may imply that shorter SPW-Rs impair memory. Our current results as well as our previous findings[25] agree with this interpretation.

The other neural features that we analyzed, TD states and PAC, were disrupted at 2WS and further disrupted at 1MS compared to controls. Disrupted TD states have been shown to cause neuroinflammation and have been associated with impairment of learning and memory[7,9,20], which may be a contributing mechanism to post-stroke cognitive impairment. PAC within the hippocampus has been shown as a mechanism for memory processing during sleep[33–35], and the breakdown of hippocampal theta rhythms, which are known to coordinate oscillations in many regions, such as entorhinal cortex and prefrontal cortex, may be a contributing factor to cognitive impairment following stroke.

EE has been shown to consistently improve behavioral measures of cognitive recovery following stroke[3,22,23]. We show that EE stabilizes the characteristics of SPW-Rs throughout stroke progression. However, TD state and PAC are further disrupted by EE following stroke. TD states, though measured in the hippocampus, are an indicator for functions of many areas of the brain. Theta-gamma coupling, which we observed within the hippocampus and between cortex and hippocampus, has also been reported between prefrontal cortex and entorhinal cortex. Therefore, the features which are further disrupted by EE are indicators of a more global effect on the brain compared to SPW-Rs, which occur locally. Interestingly, we rarely observed interaction effects between EE and stroke. This indicates that the effect that EE has on these neural features remains consistent regardless of stroke condition.

This study is limited in that our dataset consists of single time point recordings that were done under urethane anesthesia. While general anesthetics are known to reduce spike activity[36], urethane anesthesia preserves brain rhythms of interest and generates naturalistic sleep patterns[37,38]. Urethane anesthesia is widely used both in hippocampal[39] and stroke [19,40] studies. However, a single recording time point prevents assessment of neurophysiology over time and limits our observations to between-group analysis of different animals. An awake behaving recording setup will allow for a more complete understanding of how stroke affects hippocampal electrophysiology across time. Another limitation of unconscious recordings is they do not provide real-time correlates to spatial encoding or recall. An awake-behaving set-up would allow us to record electrophysiology during these events and pair them with behavioral readouts.

Stroke causes complex changes to remote regions of the brain beyond the direct infarct. Similarly, many neurological disorders have far reaching effects in remote brain regions. To create effective therapies for these disorders, a deeper understanding of how these remote regions interact is needed. Furthermore, a greater understanding of how existing therapies like EE affect these interactions is essential to developing and translating these therapies to clinical settings. Here we have shown how EE impacts SPW-Rs following stroke which may explain the cognitive improvement previously reported, however the effects on other features such as PAC require further study. PAC specifically may uncover insights that translate to other neurological disorders; for example, abnormal PAC has been implicated in Parkinson's disorder[41], Alzheimer's Disease[42], and schizophrenia[43]. This understanding will open the door for more targeted therapies as we have shown that PAC can be induced through optogenetic stimulation[44], which allows for the potential to recover PAC between regions in disease models.

Supplementary Material

Refer to Web version on PubMed Central for supplementary material.

Acknowledgments:

This project was supported by the Eunice Kennedy Shriver National Institute of Child Health & Human Development of the National Institutes of Health under Award Number K12HD073945, the Center for Neurotechnology (CNT, a National Science Foundation Engineering Research Center under Grant EEC-1028725),

NIH R01 NS102886, VA Merit Award I01BX003335 and VA Research Career Scientist award IK6BX004600. We thank Loren Frank, Kenny Kay and Karam Khateeb for advice on data analysis.

References:

[1]. Khedr EM, Hamed SA, El-Shereef HK, et al. Cognitive impairment after cerebrovascular stroke: Relationship to vascular risk factors. Neuropsychiatr Dis Treat. 2009;5(1):103–116. doi:10.2147/ndt.s4184 [PubMed: 19557105]

[2]. Bederson JB, Pitts LH, Tsuji MC, Nishimura ML, Davis RL, Bartkowski HL. Rat Middle Cerebral Artery Occlusion: Evaluation of the Model and Development of a Neurologic Examination. Stroke. 1986;17(3):472–476. doi:10.1161/01.STR.17.3.472 [PubMed: 3715945]

[3]. Wang Y, Bontempi B, Leinekugel X, et al. Environmental Enrichment Preserves Cortical Inputs to the Parahippocampal Areas and Reduces Post Stroke Diaschisis. Am J Neuroprot Neuroregen. 2011;3(1):66–76. doi:10.1166/ajnn.2011.1027

[4]. Sun C, Sun H, Wu S, et al. Conditional Ablation of Neuroprogenitor Cells in Adult Mice Impedes Recovery of Poststroke Cognitive Function and Reduces Synaptic Connectivity in the Perforant Pathway. J Neurosci. 2013;33(44):17314–17325. doi:10.1523/JNEUROSCI.2129-13.2013 [PubMed: 24174664]

[5]. de Oliveira JL, di TB Crispin P, Duarte ECW, et al. Histopathology of motor cortex in an experimental focal ischemic stroke in mouse model. J Chem Neuroanat. 2014;57–58:1–9. doi:10.1016/j.jchemneu.2014.03.002

[6]. Hazime M, Alasoadura M, Lamtahri R, et al. Prolonged deficit of gamma oscillations in the peri-infarct cortex of mice after stroke. Published online 2020. Doi:10.1101/2020.03.05.978593

[7]. Aminov A, Rogers JM, Johnstone SJ, Middleton S, Wilson PH. Acute single channel EEG predictors of cognitive function after stroke. PloS One. 2017;12(10):1–15. Doi:10.1371/journal.pone.0185841

[8]. Buzsáki G Theta oscillations in the hippocampus. Neuron. 2002;33(3):325–340. Doi:10.1016/S0896-6273(02)00586-X [PubMed: 11832222]

[9]. Williams AJ, Lu XCM, Hartings JA, Tortella FC. Neuroprotection assessment by topographic electroencephalographic analysis: Effects of a sodium channel blocker to reduce polymorphic delta activity following ischaemic brain injury in rats. Fundam Clin Pharmacol. 2003;17(5):581–593. Doi:10.1046/j.1472-8206.2003.00183.x [PubMed: 14703719]

[10]. Buzsaki G Hippocampal Sharp Wave-Ripple: A Cognitive Biomarkerfor Episodic Memory and Planning. Hippocampus. 2015;25(10). Doi:10.1002/hipo.22488

[11]. Kay K, Sosa M, Chung JE, Karlsson MP, Larkin MC, Frank LM. A hippocampal network for spatial coding during immobility and sleep. Nature. 2016;531(7593). Doi:10.1038/nature17144

[12]. Heusser AC, Poeppel D, Ezzyat Y, Davachi L. Episodic sequence memory is supported by a theta-gamma phase code. Nat Neurosci. 2016;19(10):1374–1380. Doi:10.1038/nn.4374 [PubMed: 27571010]

[13]. Tort ABL, Komorowski R, Eichenbaum H, Kopell N. Measuring phase-amplitude coupling between neuronal oscillations of different frequencies. J Neurophysiol. 2010;104(2):1195–1210. Doi:10.1152/jn.00106.2010 [PubMed: 20463205]

[14]. Tort ABL, Komorowski RW, Manns JR, Kopell NJ, Eichenbaum H. Theta-gamma coupling increases during the learning of item-context associations. Proc Natl Acad Sci U S A. 2009;106(49):20942–20947. Doi:10.1073/pnas.0911331106 [PubMed: 19934062]

[15]. Tamura M, Spellman TJ, Rosen AM, Gogos JA, Gordon JA. Hippocampal-prefrontal theta-gamma coupling during performance of a spatial working memory task. Nat Commun. 2017;8(1). Doi:10.1038/s41467-017-02108-9

[16]. Bandarabadi M, Boyce R, Herrera CG, et al. Dynamic modulation of theta-gamma coupling during rapid eye movement sleep. Sleep. 2019;42(12):1–11. Doi:10.1093/sleep/zsz182

[17]. McNaughton N, Ruan M, Woodnorth M-A. Restoring Theta-like Rhythmicity in Rats Restores Initial Learning in Morris Water Maze. Hippocampus. 2006;16:1102–1110. Doi:10.1002/hipo [PubMed: 17068783]

[18]. Schmitt O, Badurek S, Liu W, et al. Prediction of regional functional impairment following experimental stroke via connectome analysis. Sci Rep. 2017;7(12 2016):1–18. Doi:10.1038/srep46316 [PubMed: 28127051]

[19]. Rabiller G, He JW, Nishijima Y, Wong A, Liu J. Perturbation of brain oscillations after ischemic stroke: A potential biomarker for post-stroke function and therapy. Int J Mol Sci. 2015;16(10):25605–25640. Doi:10.3390/ijms161025605 [PubMed: 26516838]

[20]. Ip Z, Rabiller G, He JW, et al. Cortical stroke affects activity and stability of theta/delta states in remote hippocampal regions *. In:; 2019:5225–5228. Doi:10.1109/embc.2019.8857679

[21]. Cooper RM, and Zubek JP Effects of enriched and restricted early environments on the learning ability of bright and dull rats. Can. J. Psychol 1958; 12, 159–164. [PubMed: 13573245]

[22]. Hamm RJ, Temple MD, O'Dell DM, Pike BR, & Lyeth BG Exposure to environmental complexity promotes recovery of cognitive function after traumatic brain injury. Journal of Neurotrauma, 1996; 13(1), 41–47. [PubMed: 8714862]

[23]. Matsumori Y, Hong SM, Fan Y, et al. Enriched environment and spatial learning enhance hippocampal neurogenesis and salvages ischemic penumbra after focal cerebral ischemia. Neurobiol Dis. 2006;22(1):187–198. Doi:10.1016/j.nbd.2005.10.015 [PubMed: 16361108]

[24]. Fan Y, Liu Z, Weinstein PR, Fike JR, Liu J. Environmental enrichment enhances neurogenesis and improves functional outcome after cranial irradiation. Eur J Neurosci. 2007;25(1):38–46. Doi:10.1111/j.1460-9568.2006.05269.x [PubMed: 17241265]

[25]. He JW, Rabiller G, Nishijima Y, et al. Experimental cortical stroke induces aberrant increase of sharp-wave-associated ripples in the hippocampus and disrupts cortico-hippocampal communication. J Cereb Blood Flow Metab. Published online 2019. Doi:10.1177/0271678X19877889

[26]. Sun H, Le T, Chang TT, Habib A, Wu S, Shen F, Young WL, Sun H, Liu J. AAV-mediated netrin-1 overexpression increases periinfarct blood vessel density and improves motor function recovery after experimental stroke. Neurobiology of disease. 2011; 44:73–83. [PubMed: 21726647]

[27]. Bódizs R, Kántor S, Szabó G, Szûcs A, Erõss L, Halász P. Rhythmic hippocampal slow oscillation characterizes REM sleep in humans. Hippocampus. 2001;11(6):747–753. doi:10.1002/hipo.1090 [PubMed: 11811669]

[28]. Kay K, Sosa M, Chung JE, Karlsson MP, Larkin MC, Frank LM. A hippocampal network for spatial coding during immobility and sleep. Nature. 2016;531(7593). doi:10.1038/nature17144

[29]. Kenan-Vaknin G, Teyler TJ. Laminar pattern of synaptic activity in rat primary visual cortex: comparison of in vivo and in vitro studies employing the current source density analysis. Brain Res. 1994;635(1–2):37–48. doi:10.1016/0006-8993(94)91421-4 [PubMed: 8173978]

[30]. Otsu N A Threshold Selection Method from Gray-Level Histograms. IEEE Trans Syst Man Cybern. 1979;C(1):62–66.

[31]. Carmichael ST. Brain excitability in stroke: The yin and yang of stroke progression. Arch Neurol. 2012;69(2):161–167. doi:10.1001/archneurol.2011.1175 [PubMed: 21987395]

[32]. Fernández-Ruiz A, Oliva A, de Oliveira EF, Rocha-Almeida F, Tingley D, Buzsáki G. Long-duration hippocampal sharp wave ripples improve memory. Science (80-). 2019;364(6445):1082–1086. doi:10.1126/science.aax0758

[33]. Rasch B, Born J. About sleep's role in memory. Physiol Rev. 2013;93(2):681–766. doi:10.1152/physrev.00032.2012 [PubMed: 23589831]

[34]. Staresina BP, Bergmann TO, Bonnefond M, et al. Hierarchical nesting of slow oscillations, spindles and ripples in the human hippocampus during sleep. Nat Neurosci. 2015;18(11):1679–1686. doi:10.1038/nn.4119 [PubMed: 26389842]

[35]. Bergmann TO, Born J. Phase-Amplitude Coupling: A General Mechanism for Memory Processing and Synaptic Plasticity? Neuron. 2018;97(1):10–13. doi:10.1016/j.neuron.2017.12.023 [PubMed: 29301097]

[36]. Suzuki SS, Smith GK. Spontaneous EEG spikes in the normal hippocampus. V. Effects of ether, urethane, pentobarbital, atropine, diazepam and bicuculline. Electroencephalogr Clin Neurophysiol. 1988;70(1):84–95. doi:10.1016/0013-4694(88)90198-8 [PubMed: 2455634]

[37]. Hara K, Harris RA. The anesthetic mechanism of urethane: The effects on neurotransmitter-gated ion channels. Anesth Analg. 2002;94(2):313–318. doi:10.1213/00000539-200202000-00015 [PubMed: 11812690]

[38]. Pagliardini S, Gosgnach S, Dickson CT. Spontaneous Sleep-Like Brain State Alternations and Breathing Characteristics in Urethane Anesthetized Mice. PLoS One. 2013;8(7):1–11. doi:10.1371/journal.pone.0070411

[39]. Klausberger T, Somogyi P. Neuronal diversity and temporal dynamics: The unity of hippocampal circuit operations. Science (80-). 2008;321(5885):53–57. doi:10.1126/science.1149381

[40]. Srejic LR, Valiante TA, Aarts MM, Hutchison WD. High-frequency cortical activity associated with postischemic epileptiform discharges in an in vivo rat focal stroke model: Laboratory investigation. J Neurosurg. 2013;118(5):1098–1106. doi:10.3171/2013.1.JNS121059 [PubMed: 23413946]

[41]. Devergnas A, Caiola M, Pittard D, Wichmann T. Cortical Phase-Amplitude Coupling in a Progressive Model of Parkinsonism in Nonhuman Primates. Cereb Cortex. 2019;29(1):167–177. doi:10.1093/cercor/bhx314 [PubMed: 29190329]

[42]. Zhang X, Zhong W, Brankačk J, et al. Impaired theta-gamma coupling in APP-deficient mice. Sci Rep. 2016;6:1–10. doi:10.1038/srep21948 [PubMed: 28442746]

[43]. Barr MS, Rajji TK, Zomorrodi R, et al. Impaired theta-gamma coupling during working memory performance in schizophrenia. Schizophr Res. 2017;189:104–110. doi:10.1016/j.schres.2017.01.044 [PubMed: 28148460]

[44]. Yazdan-Shahmorad A, Silversmith DB, Sabes PN. Novel techniques for large-scale manipulations of cortical networks in non-human primates. Conf Proc. Annu Int Conf IEEE Eng Med Biol Soc IEEE Eng Med Biol Soc Annu Conf. 2018;2018:5479–5482. doi:10.1109/EMBC.2018.8513668

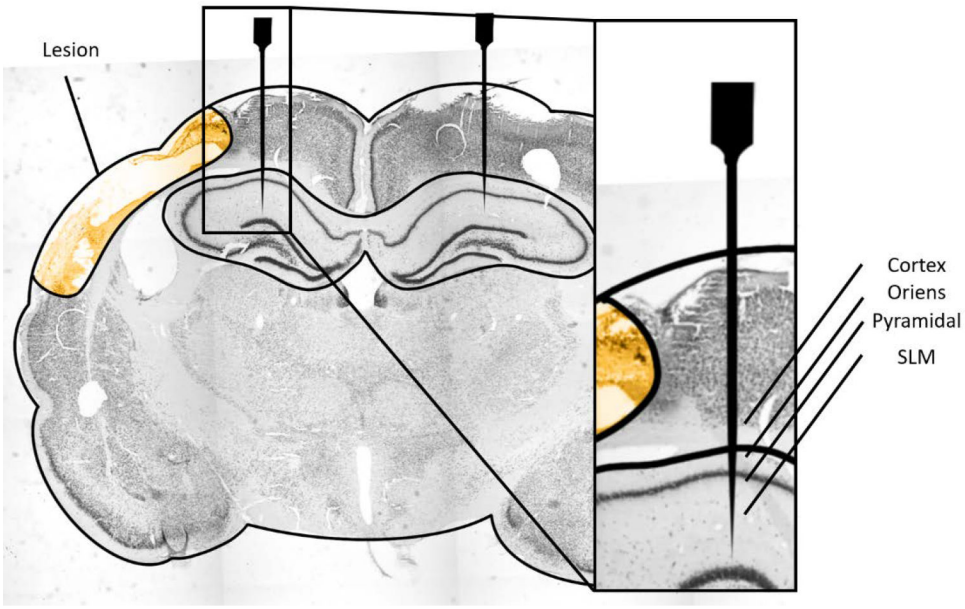

Figure 1.

Schematic of infarct area and probe locations. Probes are inserted to cover sensorimotor cortex and hippocampus. Approximate infarct and peri-infarct areas from stroke indicated by orange shading.

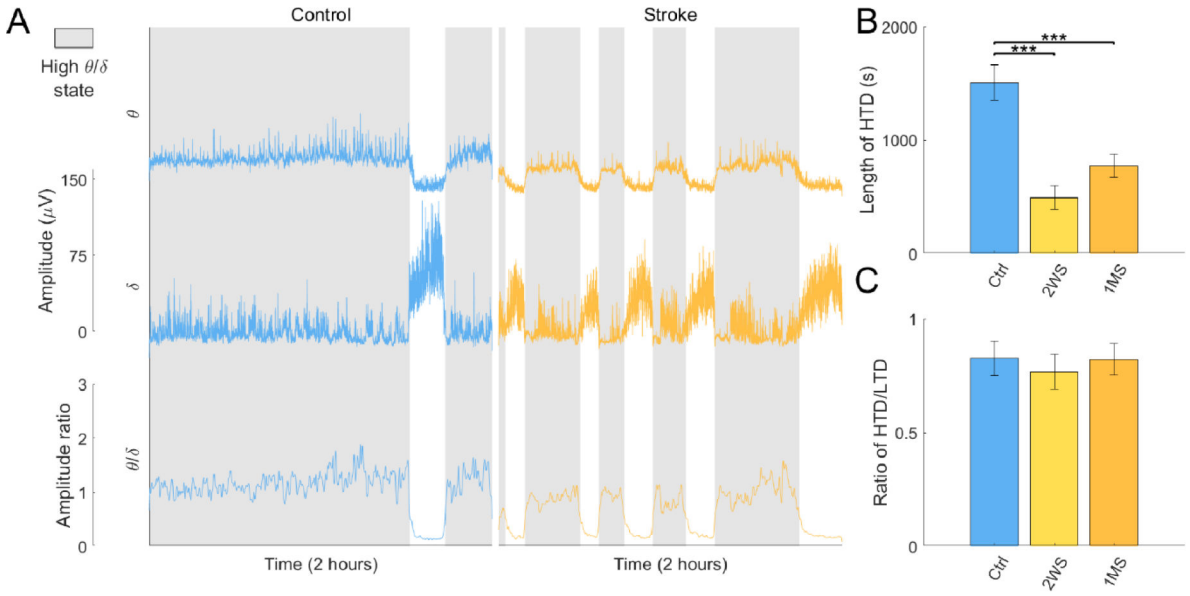

Figure 2.

Detecting HTD and LTD states. (A) The columns show examples of LFP traces for a control and stroke sample. The rows are: 1- Spontaneous amplitude of theta, 2- Spontaneous amplitude of delta, 3- Ratio of theta/delta. (B) Comparison of the average duration of ipsilateral HTD state. (C) Comparison of the proportion of ipsilesional HTD to LTD. *Significant differences ($p<0.001$, are demarked with ***).*

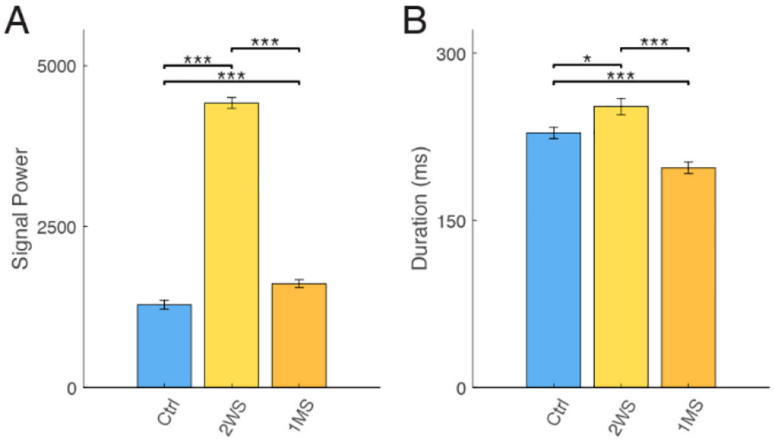

Figure 3.

Comparison of ipsilesional (A) SPW-R power and (B) SPW-R duration. *Significant differences ($p<0.05$, $p<0.01$, and $p<0.001$ are demarked with *, **, or *** respectively).*

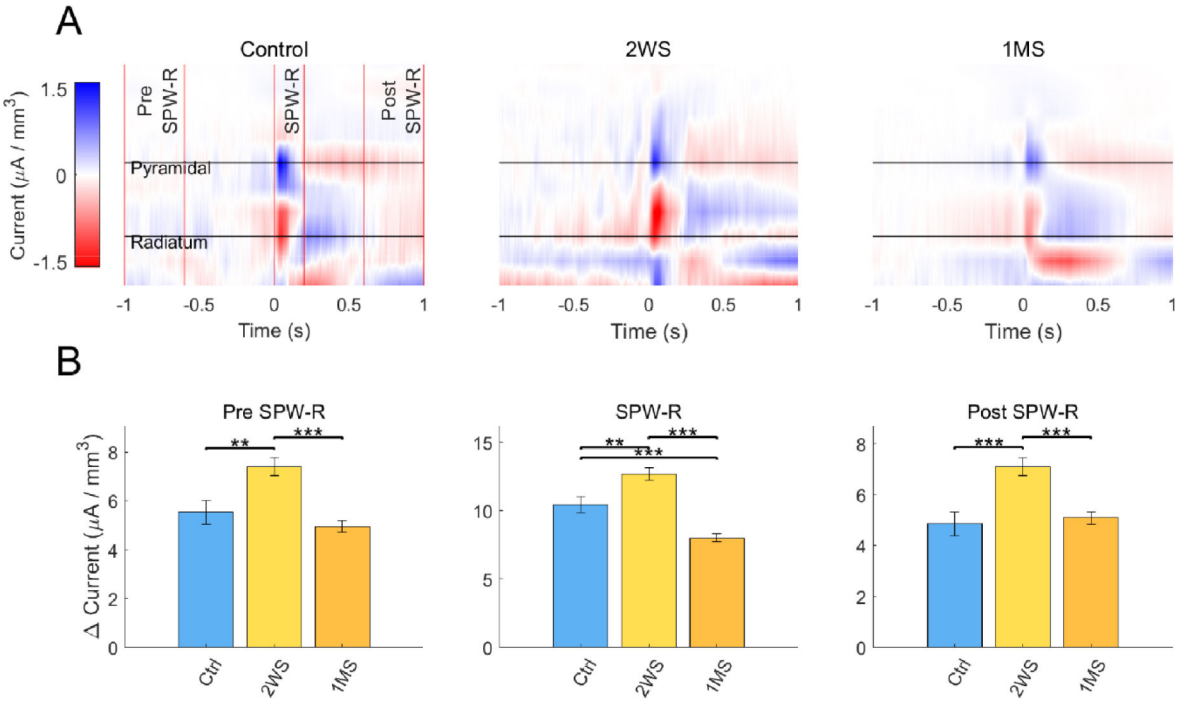

Figure 4.

Comparison of ipsilesional CSD during and following SPW-R. (A) CSD plots of ipsilesional hemisphere, displaying average current of all ripples for all animals within a particular group. Windows of interest are demarked with red lines. (B) Change in current was measured using difference between the minimum and maximum amplitudes with the demarked windows. *Significant differences: p<0.01 and p<0.001, are demarked with **, or *** respectively.*

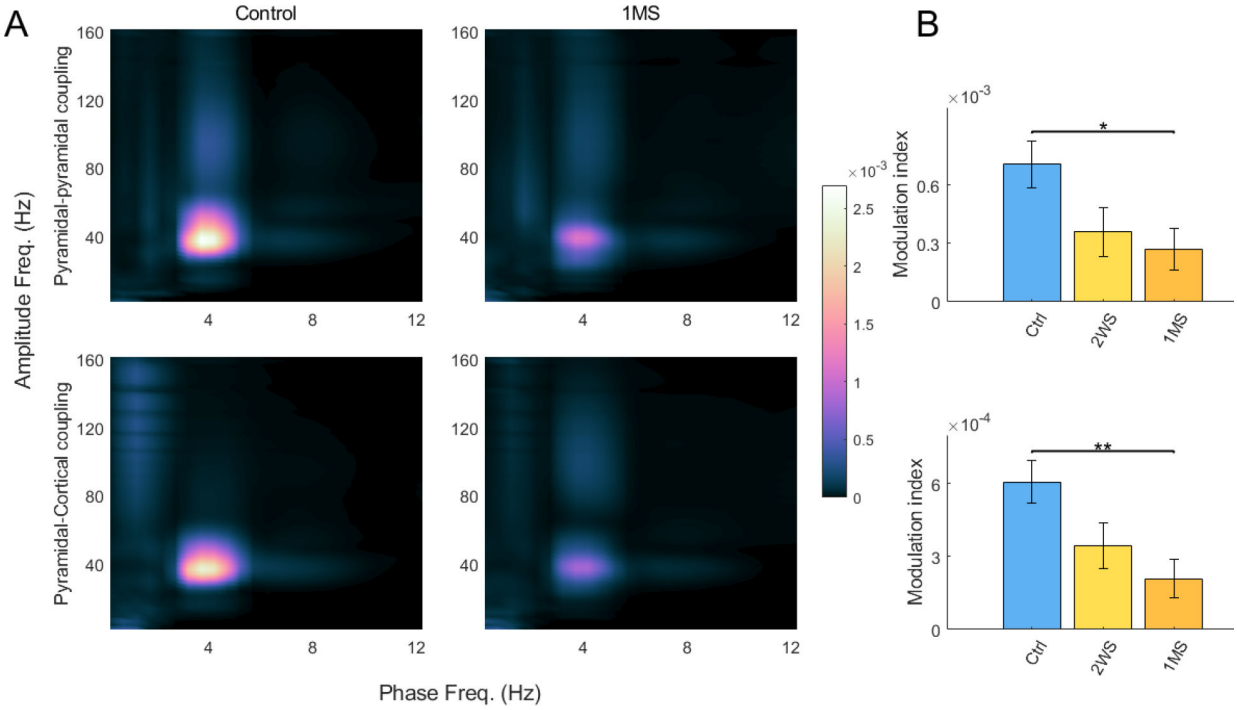

Figure 5.

Coupling between theta and gamma. (A) Phase amplitude comodulograms displaying modulation within the pyramidal layer (top), and between cortex and hippocampus (bottom). (B) Comparison of average modulation index between theta and gamma. Ipsilesional and contralesional hemispheres are compared separately. *Significant differences ($p<0.05$ and $p<0.01$, are demarked with * and ** respectively).*

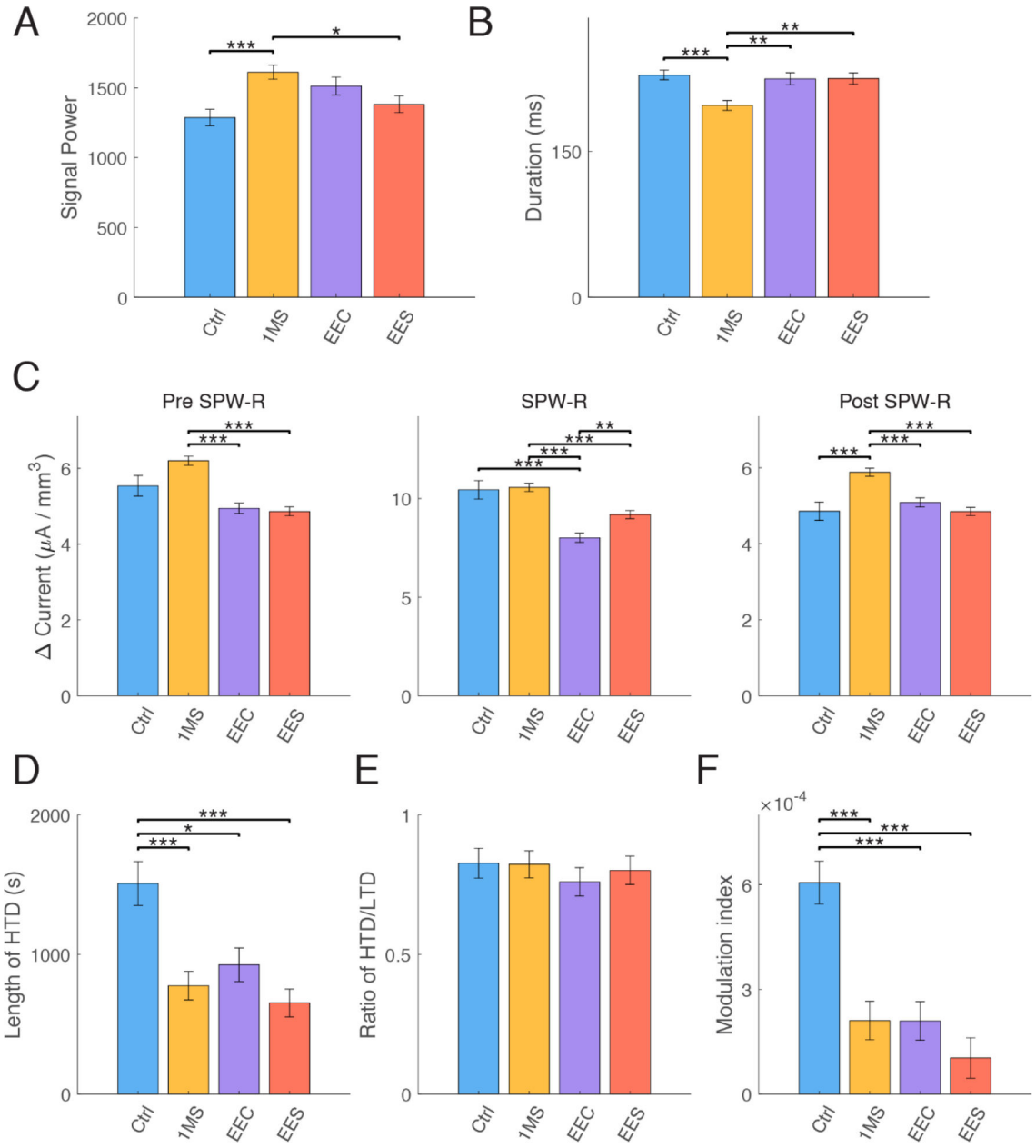

Figure 6.

Summary of the effects of EE following stroke using 2-way ANOVA comparisons on ipsilesional hemisphere. (A) Changes in SPW-R power (B) Changes in SPW-R power. (C) Changes in CSD dipole amplitude surrounding SPW-R. (D) Change in average HTD state (E) Change in HTD/LTD ratio. (F) Changes in theta-gamma coupling between cortex and pyramidal. *Significant differences: p<0.05, p<0.01 and p<0.001, are demarked with *, **, or *** respectively.*